

由含硫二羧酸配体构筑的钴(II)和锰(II) 配位聚合物的合成、晶体结构及光催化性质

黎 彧¹ 蒋汇锋¹ 成晓玲^{*2} 邱文达^{*1}

(¹广东轻工职业技术学院,广东省特种建筑材料及其绿色制备工程技术研究中心/

佛山市特种功能性建筑材料及其绿色制备技术工程中心,广州 510300)

(²广东工业大学轻工化工学院,广州 510006)

摘要: 采用水热方法,用含硫二羧酸配体 4-((carboxymethyl)thio)benzoic acid (H_2L)和 4,4'-联吡啶(4,4'-bipy)分别与 $CoCl_2 \cdot 6H_2O$ 和 $MnCl_2 \cdot 4H_2O$ 反应,合成了 2 个二维配位聚合物 $\{[Co(\mu_3-L)(4,4'-bipy)] \cdot H_2O\}_n$ (**1**)和 $\{[Mn(\mu-L)(4,4'-bipy)(H_2O)_2] \cdot H_2O\}_n$ (**2**),并对其结构和光催化性质进行了研究。结构分析结果表明 2 个配合物分别属于三斜和单斜晶系、 $P\bar{1}$ 和 $P2_1/c$ 空间群。配合物 **1** 和 **2** 分别具有基于双核 Co 和一维 Mn 链单元的二维层结构。配合物 **1** 和 **2** 具有不同的二维层结构是由于采用了不同的金属离子。另外,研究了 2 个配合物对有机染料亚甲基蓝的光催化降解性能,结果表明配合物 **2** 可以高效地降解亚甲基蓝。

关键词: 配位聚合物;二羧酸配体;光催化

中图分类号: O614.81²; O614.71¹ 文献标识码: A 文章编号: 1001-4861(2021)02-0361-07

DOI: 10.11862/CJIC.2021.028

Syntheses, Crystal Structures, and Photocatalytic Properties of Cobalt(II) and Manganese(II) Coordination Polymers Assembled from 4-((Carboxymethyl)thio)benzoic Acid

LI Yu¹ JIANG Hui-Feng¹ CHEN Xiao-Ling^{*2} QIU Wen-Da^{*1}

(¹Guangdong Research Center for Special Building Materials and Its Green Preparation Technology/Foshan Research Center for Special Functional Building Materials and Its Green Preparation Technology,

Guangdong Industry Polytechnic, Guangzhou 510300, China)

(²School of Chemical Engineering and Light Industry, Guangdong University of Technology, Guangzhou 510006, China)

Abstract: Two 2D cobalt(II) and manganese(II) coordination polymers, namely $\{[Co(\mu_3-L)(4,4'-bipy)] \cdot H_2O\}_n$ (**1**) and $\{[Mn(\mu-L)(4,4'-bipy)(H_2O)_2] \cdot H_2O\}_n$ (**2**), have been constructed hydrothermally using 4-((carboxymethyl)thio)benzoic acid (H_2L), 4,4'-bipyridine(4,4'-bipy), and cobalt or manganese chlorides. Single-crystal X-ray diffraction analyses reveal that **1** and **2** crystallize in the triclinic and monoclinic systems, space groups $P\bar{1}$ and $P2_1/c$, respectively. Complexes **1** and **2** show two different 2D sheets composed of dimer Co(II) or 1D Mn(II) chain units. The structural difference of **1** and **2** is driven by the metal(II) nodes. The photocatalytic properties of two complex were investigated, showing that **2** is a promising photocatalyst for the UV-light-driven degradation of methylene blue as a model organic dye pollutant. CCDC: 1967233, **1**; 1967234, **2**.

Keywords: coordination polymer; dicarboxylic acid; photocatalytic properties

收稿日期:2020-06-19。收修改稿日期:2020-10-28。

广东省高等职业院校珠江学者岗位计划资助项目(2015,2018)、广东省高校创新团队项目(No.2017GKCXTD001)、广州市科技计划项目(No.201904010381)、广东省高校特色创新类项目(No.2019GKTSCX010)和广东省大学生科技创新培育专项(No.pdjh2019b0690)资助。

*通信联系人。E-mail:ggcxl@163.com, qiuwd123@163.com

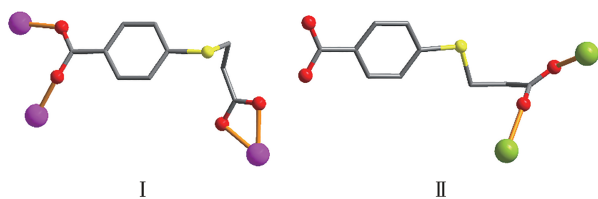
0 Introduction

Recently the field of coordination polymers have attracted a tremendous attention not only for their intriguing varieties of molecular architectures and topologies but also for their applications in catalysis, magnetism, luminescence, and gas storage^[1-5]. Although chemists and materials scientists have devoted much effort to rational design and syntheses of coordination polymers, it is difficult to predict the structures of coordination polymers, because a lot of factors influence the construction of complex, such as the structural features of organic ligands, the coordination requirements of metal ions, solvent systems, temperatures, and pH values^[6-11].

In this context, various types of aromatic polycarboxylic acids have been extensively utilized to synthesize various coordination polymers owing to their strong coordination ability in diverse modes and the fact that they are able to satisfy the geometric requirement of the metal centers^[1-2,6,12-14].

Currently, the water pollutant is becoming one serious environmental problem in the world. Much effort has been devoted to developing new photocatalytic materials for the green degradation of organic pollutants. Coordination polymers has showed good photocatalytic activities for the decomposition of organic dyes^[15-18].

As a combination of the aforementioned aspects and our previous research work, we have selected a new asymmetric dicarboxylate ligand, 4-((carboxymethyl)thio)benzoic acid (H_2L , Scheme 1) and explored it for the construction of novel coordination polymers. The ligand will not only have the characteristic coordination chemistry of the rigid carboxylate system, but also have the peculiar coordination chemistry of the



Scheme 1 Coordination modes of L^{2-} ligands in complexes **1** and **2**

flexible carboxylate system, which may be favorable for the formation of novel structures of coordination polymers. Besides, this acid block remains poorly used for the generation of coordination polymers.

In this work, we report the syntheses, crystal structures, photocatalytic properties of Co(II) and Mn(II) coordination polymers constructed from the dicarboxylate ligand.

1 Experimental

1.1 Reagents and physical measurements

All chemicals and solvents were of AR grade and used without further purification. Carbon, hydrogen and nitrogen were determined using an Elementar Vario EL elemental analyzer. IR spectra were recorded using KBr pellets and a Bruker EQUINOX 55 spectrometer. Thermogravimetric analysis (TGA) data were collected on a LINSEIS STA PT1600 thermal analyzer with a heating rate of $10\text{ }^{\circ}\text{C}\cdot\text{min}^{-1}$. Powder X-ray diffraction patterns (PXRD) were measured on a Rigaku-Dmax 2400 diffractometer using Cu $K\alpha$ radiation ($\lambda = 0.154\ 06\ \text{nm}$); the X-ray tube was operated at 40 kV and 40 mA and the data collection range was between 5° and 45° .

1.2 Synthesis of $\{[\text{Co}(\mu_3\text{-L})(4,4'\text{-bipy})]\cdot\text{H}_2\text{O}\}_n$ (**1**)

A mixture of $\text{CoCl}_2\cdot 6\text{H}_2\text{O}$ (0.048 g, 0.20 mmol), H_2L (0.049 g, 0.20 mmol), 4,4'-bipy (0.031 g, 0.20 mmol), NaOH (0.016 g, 0.40 mmol) and H_2O (10 mL) was stirred at room temperature for 15 min. Then the mixture was sealed in a 25 mL Teflon-lined stainless steel vessel, and heated at $160\text{ }^{\circ}\text{C}$ for 3 d, followed by cooling to room temperature at a rate of $10\text{ }^{\circ}\text{C}\cdot\text{h}^{-1}$. Pink block-shaped crystals of **1** were isolated manually, and washed with distilled water. Yield: 45% (based on H_2L). Anal. Calcd. for $\text{C}_{20}\text{H}_{18}\text{CoN}_2\text{O}_5\text{S}(\%)$: C 52.52, H 3.97, N 6.12; Found(%): C 52.78, H 3.99, N 6.10. IR (KBr, cm^{-1}): 3 373w, 3 059w, 1 606s, 1 550m, 1 448w, 1 408s, 1 307w, 1 279w, 1 223w, 1 172w, 1 070w, 1 015w, 935w, 845w, 817w, 772w, 733w, 693w, 631w.

1.3 Synthesis of $\{[\text{Mn}(\mu\text{-L})(4,4'\text{-bipy})(\text{H}_2\text{O})_2]\cdot\text{H}_2\text{O}\}_n$ (**2**)

The preparation of **2** was similar to that of **1** except that $\text{MnCl}_2\cdot 4\text{H}_2\text{O}$ was used instead of $\text{CoCl}_2\cdot$

6H₂O. After the reaction mixture was cooled to room temperature, yellow block - shaped crystals of **2** were isolated manually, washed with distilled water, and dried. Yield: 50% (based on H₂L). Anal. Calcd. for C₂₀H₂₂MnN₂O₇S(%): C 49.08, H 4.53, N 5.72; Found (%): C 48.86, H 4.56, N 5.70. IR (KBr, cm⁻¹): 3 160w, 2 941w, 1 699m, 1 584s, 1 532s, 1 419s, 1 369s, 1 313 w, 1 223w, 1 178w, 1 144w, 1 088w, 1 060w, 998w, 942w, 851w, 811m, 772w, 727w, 693w, 620w.

The complex are insoluble in water and common organic solvents, such as methanol, ethanol, acetone and DMF.

1.4 Structure determination

Two single crystals with dimensions of 0.23 mm×0.22 mm×0.21 mm (**1**) and 0.23 mm×0.22 mm×0.20

mm (**2**) were collected at 293(2) K on a Bruker SMART APEX II CCD diffractometer with Mo K α radiation (λ = 0.071 073 nm). The structures were solved by direct methods and refined by full matrix least-square on F^2 using the SHELXTL-2014 program^[19]. All non-hydrogen atoms were refined anisotropically. All the hydrogen atoms (except those of H₂O moieties) were positioned geometrically and refined using a riding model. The H atoms of H₂O moieties were located by difference maps and constrained to ride on their parent O atoms. A summary of the crystallography data and structure refinements for **1** and **2** is given in Table 1. The selected bond lengths and angles for complexes **1** and **2** are listed in Table 2. Hydrogen bond parameters of complexes **1** and **2** are given in Table 3.

Table 1 Crystal data and structure refinements for complexes **1** and **2**

Complex	1	2
Chemical formula	C ₂₀ H ₁₈ CoN ₂ O ₅ S	C ₂₀ H ₂₂ MnN ₂ O ₇ S
Formula weight	457.35	489.39
Crystal system	Triclinic	Monoclinic
Space group	$P\bar{1}$	$P2_1/c$
a / nm	0.962 02(11)	1.169 40(7)
b / nm	1.033 02(9)	2.084 67(13)
c / nm	1.167 18(12)	0.867 13(5)
α / (°)	91.823(8)	
β / (°)	108.270(10)	100.881(5)
γ / (°)	110.391(9)	
V / nm ³	1.019 4(2)	2.075 9(2)
Z	2	4
$F(000)$	470	1 012
θ range for data collection / (°)	3.432~25.046	3.330~25.047
Limiting indices	$-9 \leq h \leq 11, -12 \leq k \leq 12, -13 \leq l \leq 13$	$-12 \leq h \leq 13, -10 \leq k \leq 24, -10 \leq l \leq 5$
Reflection collected, unique (R_{int})	6 536, 3 605 (0.057 0)	6 592, 3 666 (0.038 7)
D_c / (g·cm ⁻³)	1.490	1.566
μ / mm ⁻¹	0.978	0.783
Data, restraint, parameter	3 605, 0, 262	3 666, 0, 280
Goodness-of-fit on F^2	1.056	1.052
Final R indices [$I \geq 2\sigma(I)$] R_1, wR_2	0.069 3, 0.108 9	0.047 9, 0.071 3
R indices (all data) R_1, wR_2	0.163 2, 0.198 9	0.099 4, 0.117 8
Largest diff. peak and hole / (e·nm ⁻³)	918 and -650	376 and -389

Table 2 Selected bond lengths (nm) and bond angles (°) for complexes **1** and **2**

1					
Co(1)—O(1)	0.201 0(4)	Co(1)—O(2)A	0.204 5(4)	Co(1)—O(3)B	0.223 3(4)
Co(1)—O(4)B	0.217 1(4)	Co(1)—N(1)	0.215 1(4)	Co(1)—N(2)C	0.214 8(4)

Continued Table 2

O(1)—Co(1)—O(2)A	119.64(18)	O(1)—Co(1)-N(2)C	91.44(17)	O(2)A—Co(1)—N(2)C	92.56(16)
O(1)—Co(1)—N(1)	88.26(17)	O(2)A—Co(1)-N(1)	87.63(16)	N(1)—Co(1)—N(2)C	179.70(17)
O(1)—Co(1)—O(4)B	149.45(17)	O(2)A—Co(1)-O(4)B	90.84(16)	N(2)C—Co(1)—O(4)B	89.12(17)
N(1)—Co(1)—O(4)B	91.11(17)	O(1)—Co(1)-O(3)B	90.48(17)	O(2)A—Co(1)—O(3)B	149.38(18)
N(2)C—Co(1)—O(3)B	91.98(17)	N(1)—Co(1)—O(3)B	87.97(17)	O(4)B—Co(1)—O(3)B	58.98(15)
2					
Mn(1)—O(1)A	0.217 9(2)	Mn(1)—O(2)	0.213 3(2)	Mn(1)—O(5)	0.214 0(2)
Mn(1)—O(6)	0.219 8(2)	Mn(1)—N(1)	0.230 2(3)	Mn(1)—N(2)B	0.229 0(3)
O(2)—Mn(1)—O(5)	177.55(9)	O(2)—Mn(1)—O(1)A	81.85(9)	O(5)—Mn(1)—O(1)A	99.56(9)
O(2)—Mn(1)—O(6)	94.18(9)	O(5)—Mn(1)—O(6)	84.59(9)	O(1)A—Mn(1)—O(6)	173.46(8)
O(2)—Mn(1)—N(2)B	87.91(9)	O(5)-Mn(1)—N(2)B	90.15(9)	O(1)A—Mn(1)—N(2)B	87.24(9)
O(6)—Mn(1)—N(2)B	97.85(10)	O(2)—Mn(1)—N(1)	92.29(9)	O(5)—Mn(1)—N(1)	89.66(9)
O(1)A—Mn(1)—N(1)	91.93(10)	O(6)—Mn(1)—N(1)	83.01(10)	N(2)B—Mn(1)—N(1)	179.11(11)

Symmetry codes: A: $-x, -y+1, -z+1$; B: $-x, -y+1, -z+2$; C: $x-1, y-1, z$ for **1**; A: $x, -y+1/2, z+1/2$; B: $x-1, y, z$ for **2**.

Table 3 Hydrogen parameters of complexes **1** and **2**

Complex	D—H···A	$d(\text{D—H}) / \text{nm}$	$d(\text{H}\cdots\text{A}) / \text{nm}$	$d(\text{D}\cdots\text{A}) / \text{nm}$	$\angle\text{DHA} / (^\circ)$
1	O(5)—H(1W)···O(3)A	0.085 0	0.203 3	0.288 3	178.91
2	O(5)—H(1W)···O(7)B	0.082 0	0.193 9	0.271 9	158.61
	O(5)—H(2W)···O(1)C	0.083 7	0.188 4	0.271 1	169.24
	O(6)—H(4W)···O(3)D	0.082 0	0.182 3	0.263 6	170.87
	O(7)—H(6W)···O(4)E	0.086 8	0.218 6	0.270 1	117.77

Symmetry codes: A: $-x, -y+1, -z+2$ for **1**; B: $-x+1, -y+1, -z+1$; C: $x, y, z+1$; D: $-x, -y, -z+1$; E: $x+1, y+1, z$ for **2**.

CCDC: 1967233, **1**; 1967234, **2**.

1.5 Photocatalytic activity studies

Photocatalytic degradation of methylene blue (MB) in the presence of catalysts **1** and **2** was investigated using a Cary 5000 UV-Vis-NIR spectrophotometer. The catalytic reactions were performed as follows: catalyst (50 mg) was dispersed in 100 mL aqueous solution of MB ($10 \text{ mg} \cdot \text{L}^{-1}$) under stirring for 30 min in the dark, aiming to ensure an adsorption-desorption equilibrium. The obtained mixture was then exposed to a continuous UV irradiation using an Hg lamp (150 W) for 150 min with continuous stirring. The reaction samples (5 mL) were taken out every 15 min, centrifuged, and then analyzed by UV-Vis spectrophotometry, monitoring an intensity decrease of the MB absorption band at 668 nm. A control experiment was also performed under the same reaction conditions, showing that no MB degradation took place in the absence of catalyst.

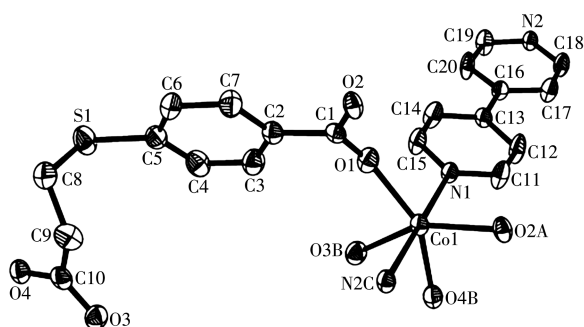
2 Results and discussion

2.1 Description of the structures

2.1.1 Structure of **1**

Asymmetric unit of **1** contains a Co1 atom, a μ_3 -L²⁻ block, a 4,4'-bipy moiety, and one lattice water molecule (Fig. 1). The six-coordinated Co1 center displays a distorted octahedral {CoN₂O₄} environment filled by four carboxylate O atoms from three individual μ_3 -L²⁻ blocks and two N atoms from two different 4,4'-bipy moieties. The lengths of the Co—O and Co—N bonds are 0.201 0(4)~0.223 3(4) and 0.214 8(4)~0.215 1(4) nm, respectively; these are within the normal values for related Co(II) derivatives^[11,11,13]. In **1**, the L²⁻ block acts as a μ_3 -ligand, wherein the COO⁻ groups are bidentate (mode I, Scheme 1). Two carboxylate groups of two μ_3 -L²⁻ blocks link the adjacent Co(II) centers into the dicobalt(II) motifs (Fig. 2) with a Co···Co separation of 0.409 2(4) nm. Such motifs are further assembled, via the remaining COO⁻ groups of μ_3 -L²⁻ blocks and 4,4'-

bipy moieties to a 2D sheet (Fig.3).

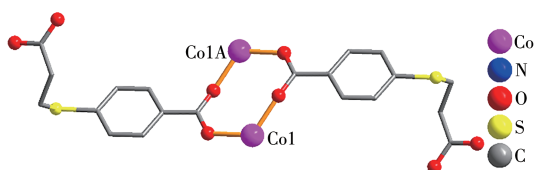


Lattice water molecule and H atoms are omitted for clarity;

Symmetry codes: A: $-x, -y+1, -z+1$; B: $-x, -y+1, -z+2$;

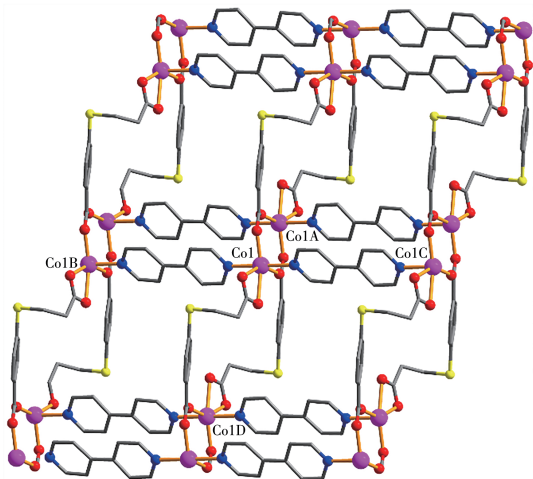
C: $x-1, y-1, z$

Fig.1 Drawing of asymmetric unit of complex **1** with 30% probability thermal ellipsoids



Symmetry code: A: $-x, -y+1, -z+1$

Fig.2 Di-cobalt(II) motif



Symmetry codes: A: $-x, -y+1, -z+1$; B: $x-1, y-1, z$; C: $x+1, y+1, z$;

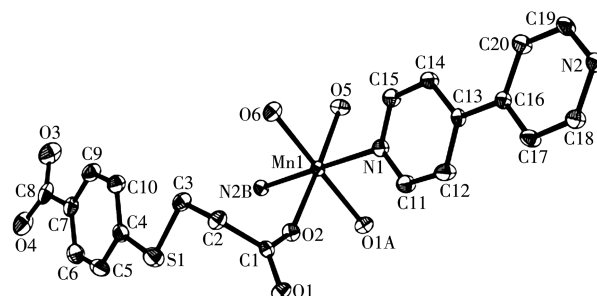
D: $-x, -y+1, -z+2$

Fig.3 View of 2D sheet in complex **1** along *b* axis

2.1.2 Structure of **2**

Asymmetric unit of **2** bears one Mn1 center, one μ -L²⁻ linker, one μ -4,4'-bipy, two terminal water ligands and one lattice water molecule (Fig.4). The Mn1 center is six-coordinated and reveals a distorted octahedral {MnN₂O₄} geometry. It is completed by two carboxylate O donors from two μ -L²⁻ blocks, two O atoms from two

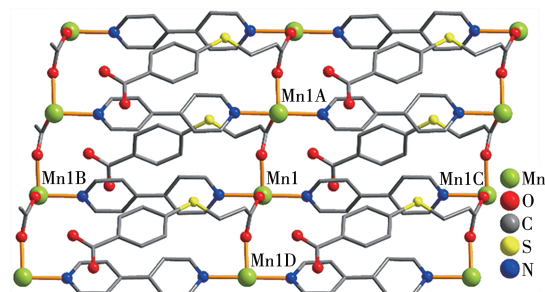
H₂O ligands, and two N donors from two independent 4,4'-bipy ligands. The Mn—O (0.2133(2)~0.2198(2) nm) and Mn—N (0.2290(3)~0.2302(3) nm) bonds are within the standard values^[6,11]. The L²⁻ block behaves as a bidentate μ -linker (Scheme 1, mode II) that interconnects the adjacent Mn1 atoms to form a 1D metal-organic chain subunit with a Mn1...Mn1 separation of 0.5198(3) nm (Fig. 5). Furthermore, such 1D chains are further extended by μ -4,4'-bipy into a 2D sheet (Fig. 5). Complexes **1** and **2** were isolated under the same conditions, except for the type of metal(II) chloride starting material (CoCl₂·6H₂O for **1** and MnCl₂·4H₂O for **2**). Hence, the structural difference between two products indicates that the assembly process is metal ion-dependent.



Lattice water molecule and H atoms are omitted for clarity; Symme-

try codes: A: $x, -y+1/2, z+1/2$; B: $x-1, y, z$

Fig.4 Drawing of asymmetric unit of complex **2** with 30% probability thermal ellipsoids



Symmetry codes: A: $x, -y+1/2, z-1/2$; B: $x-1, y, z$; C: $x+1, y, z$; D:

$x, -y+1/2, z+1/2$

Fig.5 View of 2D metal-organic sheet of **2** along *b* axis

2.2 TGA for **1** and **2**

To determine the thermal stability of complexes **1** and **2**, their thermal behaviors were investigated under nitrogen atmosphere by TGA. As shown in Fig.6, TGA curve of complex **1** shows that there was a loss of one lattice water molecule between 43 and 102 °C (Obsd.

3.6%, Calcd. 3.9%); further heating above 302 °C led to a decomposition of the dehydrated sample. Complex **2** lost its two H₂O ligands and one lattice water molecule in a range of 103~156 °C (Obsd. 11.3%, Calcd. 11.0%), followed by the decomposition at 158 °C.

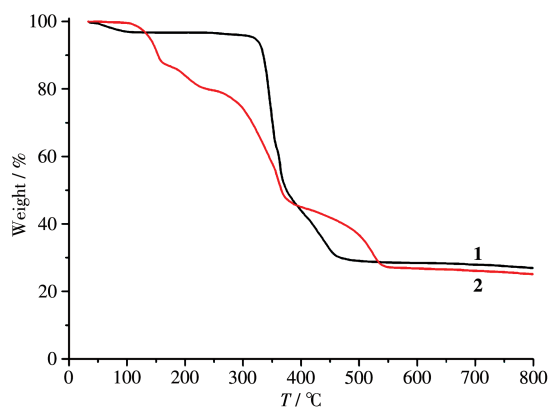


Fig.6 TGA curves of complexes **1** and **2**

2.3 Photocatalytic activity for dye degradation

To study the photocatalytic activity of **1** and **2**, we selected MB as a model dye contaminant in wastewater. The obtained results (Fig.7 and 8) indicated that the MB degradation efficiency attained 86.9% after 150 min in the presence of **2** that was the most active catalyst. For **1**, the MB degradation efficiency was inferior, being 66.0%. Under similar conditions, blank test showed that the MB degradation efficiency was only 11.6% after 150 min. Besides, to evaluate the stability of complex **2** during the photocatalytic experiments, the catalyst recycling tests were performed (Fig.9). The obtained results indicate that the complex **2** preserved

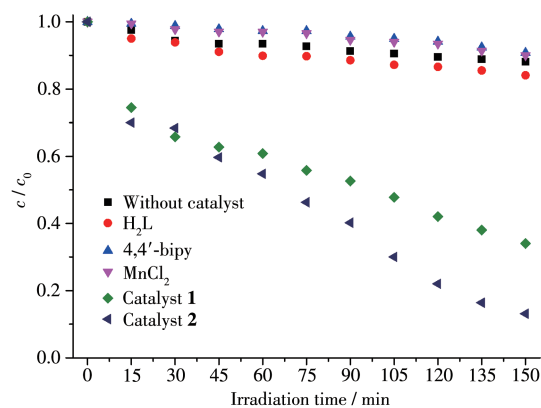


Fig.7 Photocatalytic degradation of MB solution under UV light using catalysts **1** and **2** and the blank experiment

its original catalytic activity even after four reaction cycles, showing only a slight decline of the MB degradation efficiency from 87% to 82%. Moreover, the chemical stability of **2** after photocatalytic experiments can be confirmed by the PXRD data of the recovered catalyst (Fig.10), which well matched those of as-synthesized sample. The results demonstrate that the photocatalytic activity depends on various factors, such

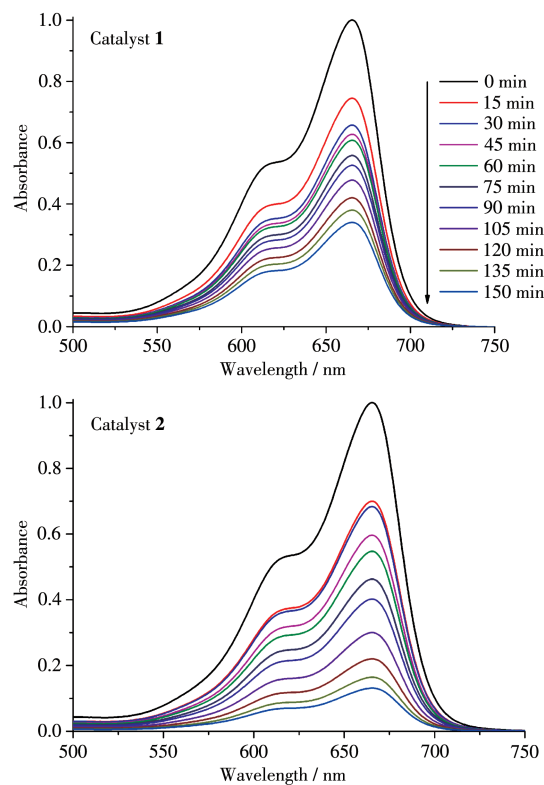


Fig.8 Time-dependent UV-Vis spectra of the reaction mixtures in the course of MB photodegradation catalyzed by **1** and **2**

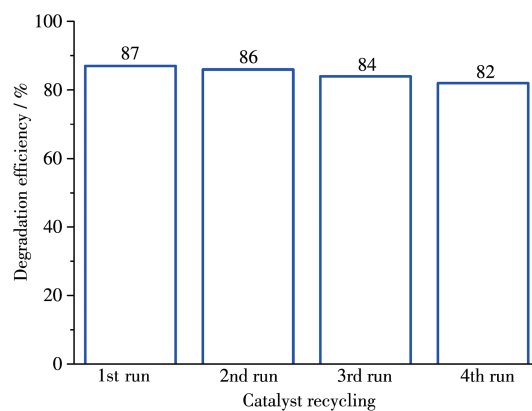


Fig.9 Catalyst **2** recycling experiments in MB photodegradation

as number of water ligands, coordination environment of metal centers, and optical band gap^[20-22].

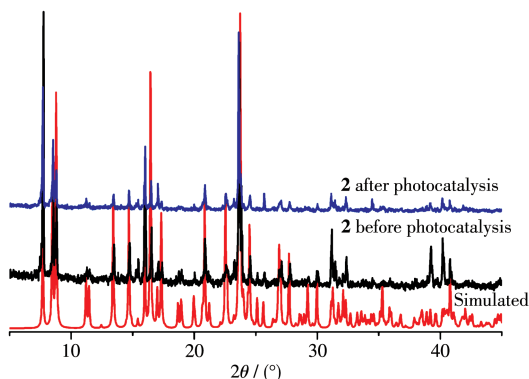


Fig.10 PXRD patterns for **2**: simulated, before and after photocatalysis

3 Conclusions

In summary, we have successfully synthesized and characterized two new cobalt and manganese coordination polymers by using one dicarboxylate acid as ligand under hydrothermal condition. Complexes **1** and **2** possess two different 2D sheet structures. The structural diversity of complexes **1** and **2** is driven by the metal (II) node. Besides, the photocatalytic properties were also investigated and discussed. The results show that such dicarboxylic acid can be used as a versatile multifunctional building block towards the generation of new coordination polymers.

References:

- [1] Gu J Z, Wen M, Cai Y, Shi Z F, Nesterov D S, Kirillova M V, Kirillov A M. *Inorg. Chem.*, **2019**,**58**(9):5875-5885
- [2] Gu J Z, Wen M, Cai Y, Shi Z F, Arol A S, Kirillova M V, Kirillov A

M. *Inorg. Chem.*, **2019**,**58**(4):2403-2412

- [3] Espallargas G M, Coronado E. *Chem. Soc. Rev.*, **2018**(2),47:533-557
- [4] Cui Y L, Yue Y F, Qian G D, Chen B L. *Chem. Rev.*, **2012**,**112**(2):1126-1162
- [5] Zou L F, Yuan J Q, Yuan Y, Gu J M, Li G H, Zhang L R, Liu Y L. *CrystEngComm*, **2019**,**21**(21):3289-3294
- [6] Gu J Z, Cui Y H, Liang X X, Wu J, Lv D Y, Kirillov A M. *Cryst. Growth Des.*, **2016**,**16**(8):4658-4670
- [7] Zhai Z W, Yang S H, Luo P, Li L K, Du C X, Zang S Q. *Eur. J. Inorg. Chem.*, **2019**(22):2725-2734
- [8] Sánchez-Férez F, Bayés L, Font-Bardia M, Pons J. *Inorg. Chim. Acta*, **2019**,**494**:112-122
- [9] 邹训重, 吴疆, 顾金忠, 赵娜, 冯安生, 黎彧. *无机化学学报*, **2019**,**35**(9):1705-1711
- ZOU X Z, WU J, GU J Z, ZHAO N, FENG A S, LI Y. *Chinese J. Inorg. Chem.*, **2019**,**35**(9):1705-1711
- [10] Li Y, Wu J, Gu J Z, Qiu W D, Feng A S. *Chin. J. Struct. Chem.*, **2020**,**39**(4):727-736
- [11] Gu J Z, Gao Z Q, Tang Y. *Cryst. Growth Des.*, **2012**,**12**(6):3312-3323
- [12] Wang H L, Zhang D P, Sun D F, Chen Y T, Wang K, Ni Z H, Tian L J, Jiang J Z. *CrystEngComm*, **2010**,**12**(4):1096-1102
- [13] 顾文君, 顾金忠. *无机化学学报*, **2017**,**33**(2):227-236
- GU W J, GU J Z. *Chinese J. Inorg. Chem.*, **2017**,**33**(2):227-236
- [14] Gu J Z, Wen M, Liang X X, Shi Z F, Kirilliva M V, Kirillov A M. *Crystals*, **2018**,**8**:83
- [15] Gu J Z, Cai Y, Wen M, Shi Z F, Kirillov A M. *Dalton. Trans.*, **2018**,**47**(40):14327-14339
- [16] Gao Q, Xu J, Bu X H. *Coord. Chem. Rev.*, **2019**,**378**:17-31
- [17] Zhao Z F, Cong B W, Su Z H, Li B R. *Cryst. Growth Des.*, **2020**,**20**(4):2753-2760
- [18] Qin L, Hu Q, Zheng Q M, Dou Y, Yang H, Zheng H G. *CrystEngComm*, **2020**,**22**(13):2327-2335
- [19] Spek A L. *Acta Crystallogr. Sect. C*, **2015**,**C71**(1):9-18
- [20] Meng X M, Zhang X, Qi P F, Zong Z A, Jin F, Fan Y H. *RSC Adv.*, **2017**,**7**(9):4855-4871
- [21] Zhang J, Wang C C. *J. Mol. Struct.*, **2017**,**1130**:223-230
- [22] Paul A K, Karthik R, Natarajan S. *Cryst. Growth Des.*, **2011**,**11**(11):5741-5749